JPEDAV (2007) 28:2–8
DOI: 10.1007/s11669-006-9015-4
1547-7037 ©ASM International

Thermodynamic and Microstructural Modeling of Nb-Si Based Alloys

Sundar Amancherla, Sujoy Kar, Bernard Bewlay, Yang Ying and Austin Chang

(Submitted November 6, 2006)

Nb-Si alloys have gained much attention over the last decade as the next generation alloys for high-temperature aero-engine applications due to their low density and improved mechanical properties. However, the microstructures of these alloys are quite complex and vary significantly with the addition of elements such as Ti and Hf. Hence, an improved understanding of the phase stability and the microstructural evolution of these alloys is essential for alloy design for advanced high-temperature applications. In the present paper, we describe the microstructural evolution modeling results of the dendritic and eutectic solidification of the binary Nb-16 at.% Si alloy, obtained using a Phase-Field simulations performed with MICRESS. The effect of parameters; such as heat extraction rate, the ratio of the diffusivity of the solute in liquid to solid, and the interfacial energy of liquid and solid interface, on the microstructural evolution during dendritic solidification is discussed in detail.

Keywords dendritic solidification, eutectic solidification, Niobium silicides, Phase-Field modeling

1. Introduction

Nb-Si based composites have been regarded as potential new materials for aero-engine components.[1–6] Recent research in Nb-Si composites has explored a variety of alloying additions such as Ti, Hf, Cr, Mo[7–9] both from the perspective of understanding phase stability of Nb solid solution, and the Nb_5Si_3 phase, as well as balancing mechanical properties. For an accelerated understanding of the phase stability of these Nb-Si alloys, it is essential to develop the accurate thermodynamic database for the prediction of phase stability. There has been a significant progress in the thermodynamic assessment of the various ternary and quarternary alloy systems such as Nb-Si-Ti, Nb-Si-Hf, Hf-Si-Ti, Cr-Si-Ti, and Nb-Si-Ti-Hf (Ref 10 and Y. Yang and Y.A. Chang, unpublished results, 2003–2005). Using these assessments, it is possible to understand the phase stability of various phases and tailor the compositions for required phase fields.

The other important aspect that influences the mechanical properties of these alloys is the microstructure itself that evolves during casting of these alloys. The as-cast microstructure has a bearing on the phase stability and thermodynamics, however, does depend on the cooling rate and other processing parameters, and is affected by the composition itself. Hence, a means for prediction of microstructural evolution during solidification in these alloys would be of a very high significance in the development of understanding of the mechanical behavior. Phase-Field modeling[11] has been used for modeling of the microstructural evolution. The current article describes the modeling of microstructural evolution of the simple binary Nb-16 at.% Si alloy as a function of cooling rate and other parameters such as the ratio of diffusivity of Si in Nb(Si) solid solution to the liquid. The Nb-16 at.% Si alloy was selected because it is the basis for more complex alloys of greater engineering relevance. The alloy can be regarded as a representative of hypo-eutectic binary alloys. In the present study, the Phase-Field modeling was performed using the software MICRESS,[12] a multicomponent, multiphase Phase-Field modeling tool. This is an important upcoming tool that is transitioning from being at academic research level to being applied to understand the materials and processes behavior to be able to select compositions or tune the process as per requirement.

2. Phase-Field Modeling of Solidification

Phase-Field models have been used and further developed in the recent past[13–15] to simulate complex interfacial patterns during solidification.[16–18] The attraction of the Phase-Field method is in the fact that the explicit tracking of the interface is completely avoided. Explicit computation of interface curvatures and normals, as done in the level-set method,[19] is also avoided in the Phase-Field method. This is achieved by solving the evolution equations of the Phase-Field variables. The Phase-Field method is a diffuse interface method, and can be reduced to a sharp interface

Sundar Amancherla and **Sujoy Kar,** GE Global Research, Bangalore 560066, India; **Bernard Bewlay,** GE Global Research, Niskayuna, NY 12309, USA; and **Yang Ying** and **Austin Chang,** Department of Materials Science & Engineering, University of Wisconsin, Madison, WI 53706, USA. Contact e-mail: Sundar_Amancherla@geind.ge.com

method in the limit of the interface thickness going to zero.[20] The quality of the solution depends on the interface thickness. In the present work the quality of the numerical solution as a function of interface thickness in relation to grid spacing has not been characterized. However, from the recent work reported on Phase-Field models for solidification,[17, 21] it has been shown that the interface thickness must be smaller than the capillary length for the solution to converge to the sharp interface limit. This was reexamined by Karma and Rappel[15] where they reported coefficients for the so-called thin-interface limit of the Phase-Field equation. In the thin-interface limit, the interface thickness only needs to be small compared to the ''mesoscale'' of the heat and/or solute diffusion field, and the classical interface conditions are satisfied for a finite thickness. Their analysis allowed for the first time fully resolved computations to be made for three-dimensional dendrites with arbitrary interface kinetics.[22]

MICRESS is based on the multiphase field model reported by Steinbach and co-workers.[23] MICRESS uses ThermoCalc's TQ interface with ThermoCalc software to calculate the thermodynamic quantities from the database that are then used for the calculation of molar Gibbs energies, and hence chemical potentials to calculate the driving force at the diffusing interface for the motion of the interface. A successful application of the model to multicomponent directional solidification in Ni-based alloys has also been reported recently.[24] This work indicated that the oscillations that occur in the solidification velocity and in the concentration profiles of the components depend on the pulling speed as well as the alloy composition. The form of the Phase-Field free energy functional in MICRESS is such that it allows for the multicomponent multiphase representation quite easily. Much work on the solidification modeling using the Phase-Field method has concentrated on complex morphologies of dendritic solidification[25] in relation to the process parameters coupled with the fluid flow[26] without independency on the eutectic solidification.[27] MICRESS does have the capability to address both dendritic and eutectic solidification processes in the same simulation owing to its versatility in modeling multiple phase transformations.

In the present study, MICRESS has been used to simulate the microstructural evolution during solidification of a binary Nb-16 at.% Si alloy. The hypo-eutectic alloy composition proceeds with dendritic solidification of an Nb(Si) solid solution until the eutectic temperature is reached, where the solidification proceeds via the eutectic reaction giving Nb_3Si and Nb(Si) eutectic. The Nb_3Si phase further undergoes eutectoid reaction into Nb_5Si_3 and Nb(Si). The eutectoid reaction being sluggish, results in the three-phase microstructure in the binary alloy. The present work is limited to the binary alloy with 16 at.% Si that results in the calculated values of eutectic temperature of 1917.8 °C and the eutectic composition of 17.5 at.% Si using the ternary thermodynamic database.[10] The model has been applied to dendritic and eutectic solidification of the present alloy to study the evolution of the Nb(Si) and Nb_3Si phases in the microstructure, and the results are presented in this article.

3. Results and Discussion

3.1 Dendritic Solidification in Nb-16 at.% Si

The dendritic morphology obtained during solidification is affected by various physical parameters such as heat extraction from the system domain, ratio of solute diffusivity in liquid to solid, and the interfacial energy between the solid and the liquid. The effect of these parameters will be discussed in this section. Separate 400×400 and 200×200 grid-calculation-domains with grid spacing of 0.05 μm have been used for the solidification microstructure modeling.

The nucleation in MICRESS has been modeled as either an effect of kinetic undercooling that can be applied to homogeneous nucleation or a seed density model following a particular site distribution for a heterogeneous nucleation. The nuclei may be off equilibrium in Phase-Field description and hence a very small critical radius may result in dissolution. Hence the curvature effect is turned off till the nuclei have reached a stable size. This process would need the minimum under-cooling that is needed for a nucleation event as an input. The model described above could be used very effectively in the cases where there is continuous growth as in the case of directional solidification. In cases where the critical nucleus size is much smaller than that of the grid spacing, the curvature parameter in the Phase-Field model that is a function of the Phase-Field variables is often replaced by an analytical model that would depend on the distance between the nuclei in space.[28]

The seed density model[28] is more often used in the cases of heterogeneous nucleation where inoculants are added as sites for heterogeneous nucleation. The nucleation sites follow a designated size distribution in time. First the biggest particles nucleate as heat is extracted at a radius specified undercooling. As they start growing and releasing latent heat they immediately start interacting with other potential nucleation precursors. Depending on the heat extraction rate and the number and sizes of all the other seeding particles, the temperature will drop more or less well below the liquidus temperature thereby defining the number of seeds that will be activated.

In this present study, the former nucleation model is used.

3.1.1 Effect of Heat Extraction Rate from the System. In the present simulation series, the latent heat of different phases has been taken into account; the effect of temperature is evaluated by the global interaction of latent heat and heat extraction. There is no temperature gradient in the calculation domain. Figure 1 shows the time evolution of the dendrites of Nb(Si) phase plotted as a function of Si in the system, where the start of under-cooling is specified to be 10° and the heat extraction rate is 300×10^6 J/m^3/s. Figure 1 also shows the evolution of temperature and volume fraction of Nb(Si) phase during solidification.

The effects of heat extraction from the system on dendrite morphology and branching were investigated. Simulations were performed using 11 nucleation sites of the Nb(Si) phase in the melt for the three cases of heat extraction rate values (100×10^6, 300×10^6 and 1000×10^6 J/m^3/s). Figure 2(a) shows the microstructures for the three

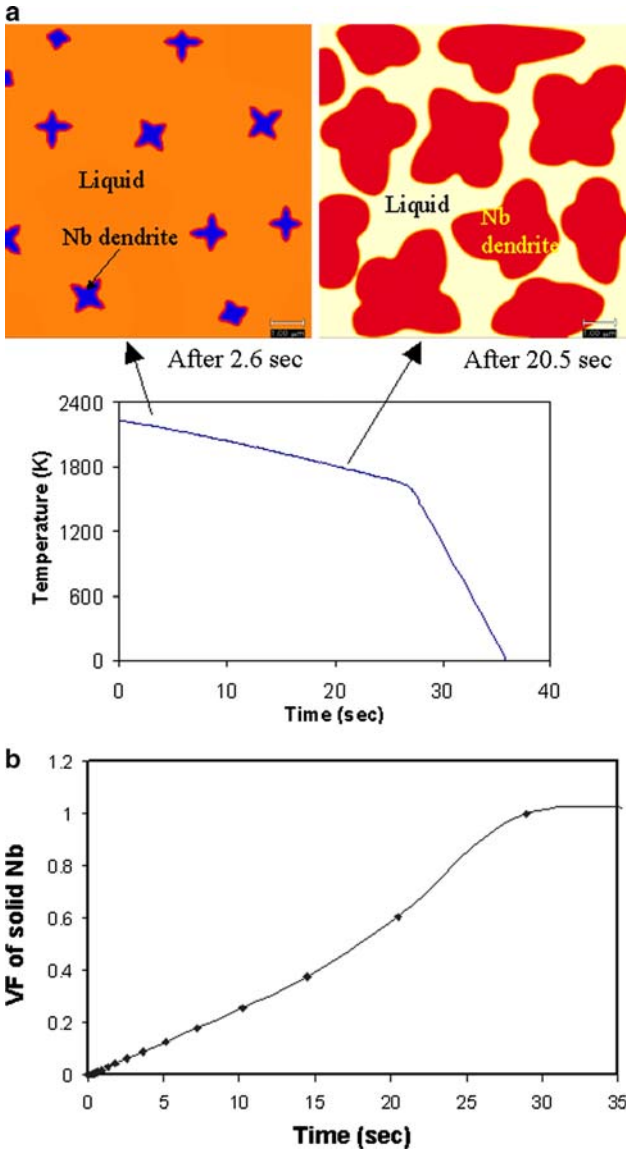

Fig. 1 Time evolution of Nb dendrites in liquid Nb-16 at.% Si. The heat extraction rate is 300×10^6 J/m^3/s

cases of heat extraction values after 25% of the Nb(Si) phase has been solidified. Figure 2(b, c) shows the associated temperature and volume fraction evolution. Figure 2 suggests that higher heat extraction causes higher tendency for front instability leading to more secondary dendritic arm formation and higher solidification rate, which seems to agree with the experimental observations of dendritic solidification reported in the literature.

3.1.2 Effect of Ratio of Solute Diffusivity in Liquid to That in Solid. The Si diffusivity in the solid Nb phase has a significant effect on secondary dendrite arm formation on primary dendrites and also on the concentration gradient of solute from core to the periphery of the dendrite. To study this effect, two ratios of the Si diffusivity in liquid to solid Nb(Si) are considered—10 and 100. The composition profiles along a line across the dendritic microstructures are extracted from two different heat extraction rates (200×10^6 and 300×10^6 J/m^3/s), for these diffusivity ratios. Figure 3 shows a case where the ratio of diffusivities has been maintained at a value of 10. The associated composition profile does not show any coring effect (concentration gradient caused due to solidification of enriched liquid resulting in a lower solute content at the core of the dendrite) due to change in heat extraction rate. This could be due to the higher solute diffusivity in the solid. Typically, the solute diffusivity in the solid is close to two orders of magnitude lower than that in the liquid phase.

For the case of the ratio of diffusivities being 100 coring does occur as there is not enough time allowed at higher temperature for diffusion to occur. Figures 4 and 5 show this effect explicitly. Figure 4 shows one dendrite column growing from the corner of the simulation domain at an angle of 45°. The case with solute diffusivity ratio of 10 in liquid to solid does not show a color gradient from the core of the dendrite to the interface. However, the case of slow Si diffusivity shows the concentration gradient which indicates coring. The same behavior is also observed in simulations with multiple dendritic seeds as shown in Fig. 5. The composition profiles along the lines across the same dendrite for the cases of high and low solute diffusivity in solid are shown in Fig. 5. The tendency of formation of side branches is also related to the solute diffusivity ratio in liquid to solid. As seen in Fig. 4(b), faster diffusion of the solute in solid phase causes reduced segregation which in turn reduces the tendency of the solid front instability, as a result of which faster Si diffusivity in solid phase lowers the tendency of formation of side branches from dendrites.

3.1.3 Effect of Interfacial Energy Between Liquid and Solid. Solid/liquid interfacial energy does influence the evolution of the morphology of the solidifying dendritic phase. For the case of a lower interfacial energy, the system will try to increase the surface area causing more branching in the dendritic morphology. This is evident in Fig. 6. The growth velocity or mobility of the interface also has an effect on side branch formation and front stability. While low mobility of the interface causes less tendency to form dendritic side branches, high growth velocity can cause front instability and disintegration of the solidification front. The parameters that were chosen are based on the fact that the surface energies of some of the metallic materials are in the range of 10-100 mJ/m^2. Another important factor is the anisotropy in the interfacial energy of the solid-liquid interface. The anisotropy of the solid-liquid interface does influence the stability and the morphology of the tips of the dendrites.[25] The effect of the anisotropy and its sensitivity toward the overall solidification process have not been rigorously characterized in the present study.

3.2 Dendritic and Eutectic Solidification in Nb-16 at.% Si

The binary Nb-Si phase diagram contains an eutectic, $L \rightarrow Nb_3Si + Nb$ at 1917.8 °C. The eutectic occurs at 17.5 at.% Si as calculated using the ternary thermodynamic database. In this solidification simulation of the hypo-eutectic alloy Nb-16 at.% Si, the Nb dendrites are formed as the primary phase until the system reaches a given under-

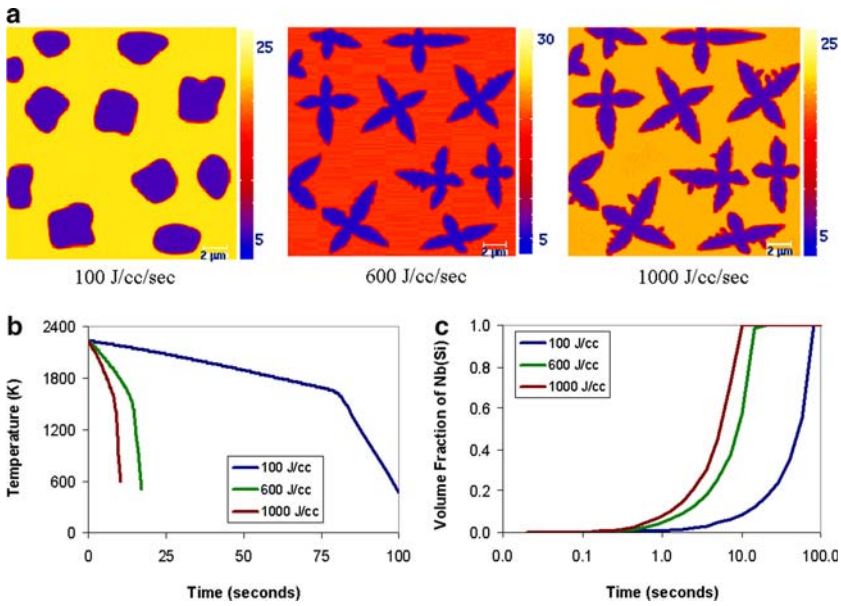

Fig. 2 (a) Effect of heat extraction rate on dendritic morphology at fixed volume fraction. Finer structures result with the increased heat extraction rates. (b) Temperature versus time. (c) Volume fraction of solid Nb phase versus time

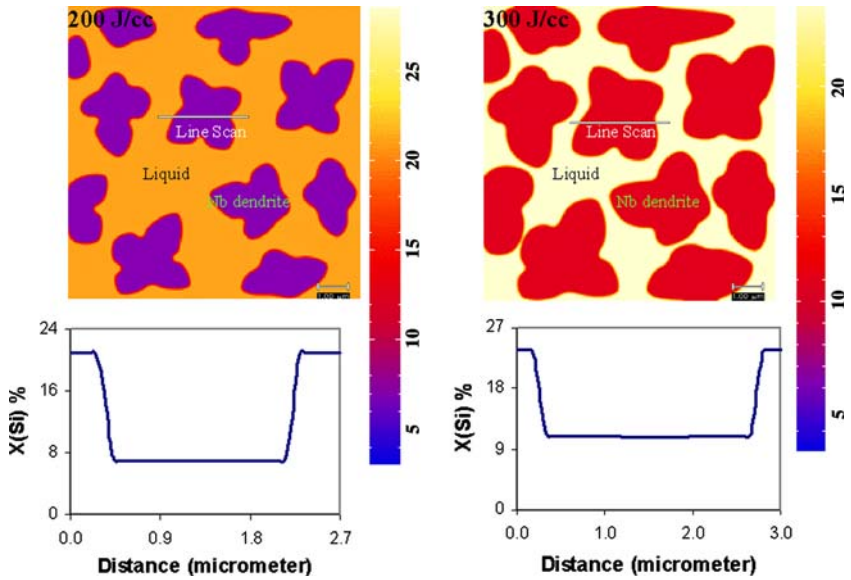

Fig. 3 Dendritic solidification microstructures solidified at the heat extraction rates of 200×10^6 J/m^3/s and 300×10^6 J/m^3/s

cooling (10 °C) below eutectic temperature, when the remaining liquid attains the eutectic composition. At that point, the eutectic microstructure nucleates and grows from the dendrite-liquid interface. Figure 7 shows the microstructure evolution at an intermediate time 21 s. In this case, a heat extraction rate is 45×10^6 J/m^3.

In the simulation, the Nb(Si) phase has been considered as an anisotropic phase (i.e., the interfacial energy is anisotropic) and the eutectic Nb_3Si particles of faceted shapes with <110> type facets and with kinetic anisotropic factor of 0.5 for each facet. This parameter represents a factor that would increase the surface energy in a preferred direction and decrease the mobility in other directions. Depending on the isotropic or anisotropic or faceted nature of the phases, and on different process parameters, there can be different morphologies of the eutectic microstructure. The typical value that would suit most alloy systems (private communication with MICRESS support group) would be between 0 and 0.5. For example, it can be lamellar growth of two phases, or one phase can be rod shaped in the matrix of the other phase. In either case, both the phases grow continuously from the melt. The volume fraction of

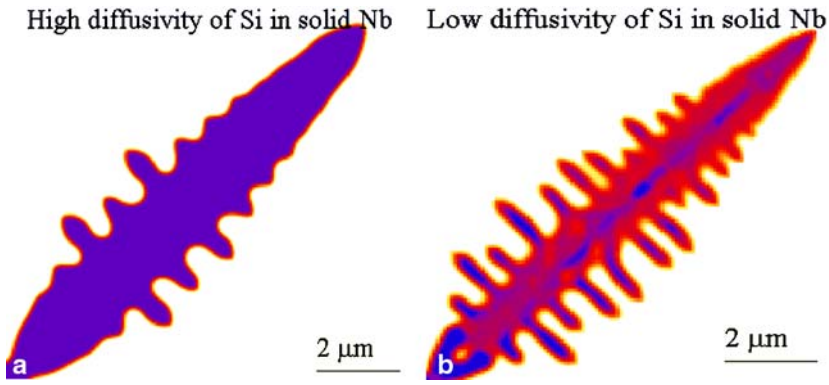

Fig. 4 Effect of diffusivity of Si on dendritic morphology. (a) High, (b) Low diffusivity in solid Nb(Si). Lower diffusivity results in higher tendency for branching and also coring (can be observed as the concentration gradient from core of the dendritic arm towards the solid solid-liquid interface)

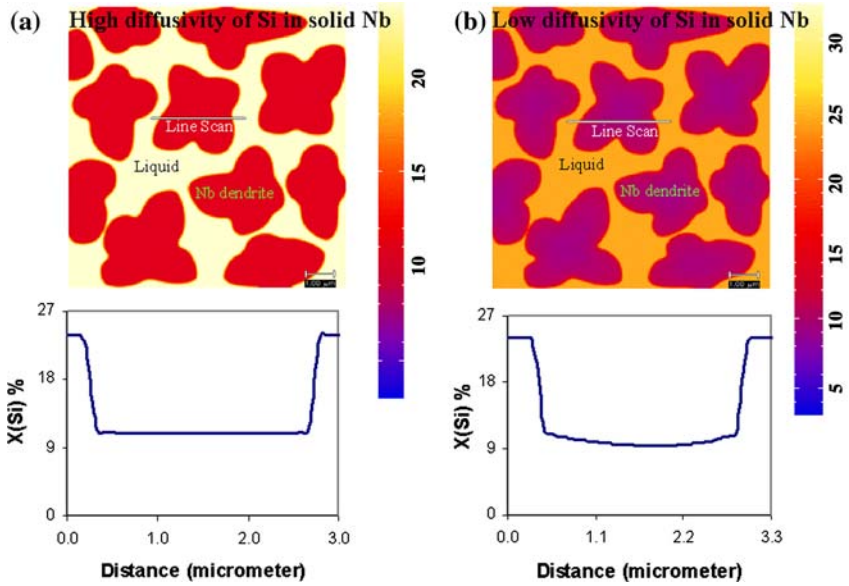

Fig. 5 (a) Effect of high diffusivity of Si in solid Nb. (b) Low diffusivity of Si in solid Nb. Note: The coring effect in the case of lower diffusivity of the solute in solid dendrite phase

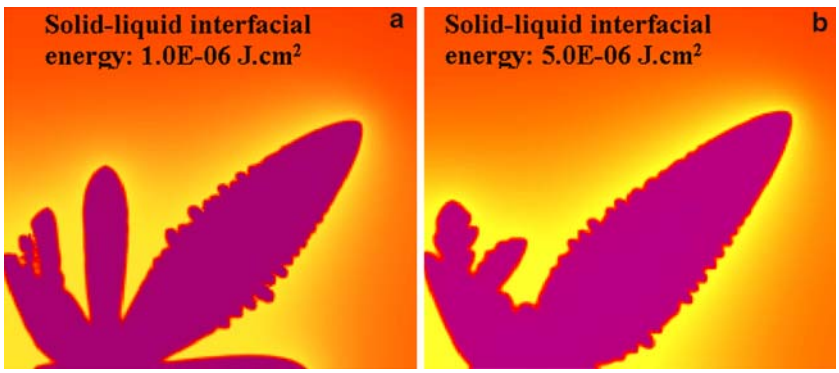

Fig. 6 Effect of solid-liquid interfacial energy on dendritic morphology: (a) lower interfacial energy, and (b) higher interfacial energy. More branching appears when interfacial energy is lower in (a)

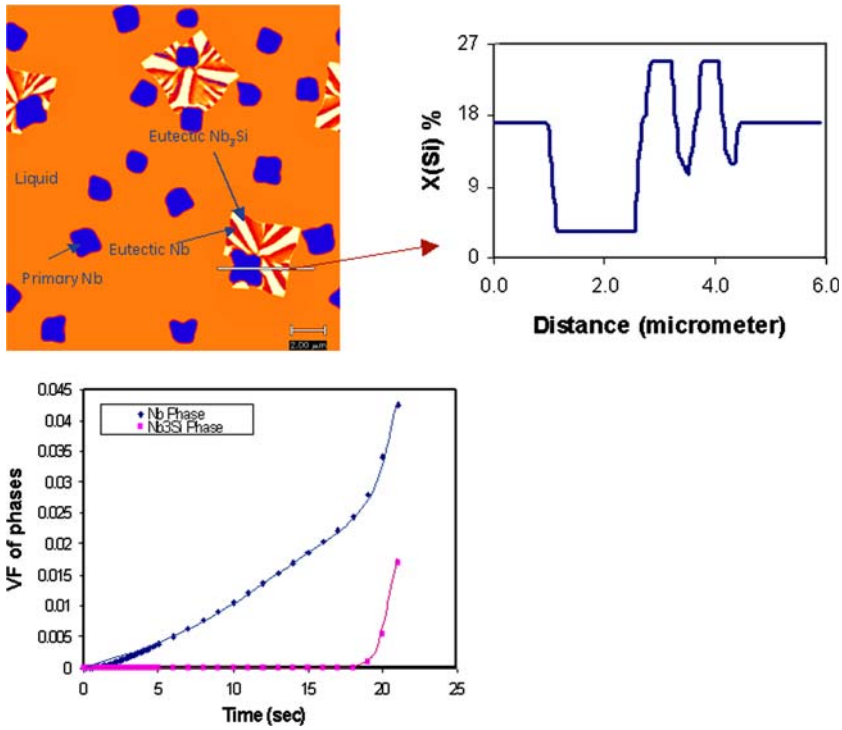

Fig. 7 Dendritic and Eutectic solidification simulation of the Nb-16 at.% Si alloy. The composition profile of Si is shown across the dendrite and the eutectic structure in the bottom half of the microstructure. The associated change in the slope of the volume fraction versus time graph should be noted after 19 s that marks the start of the eutectic solidification

the Nb_3Si under fully solidified condition is around 50% in the present alloy—Nb-16 at.% Si. Experimental observation shows that for hypo-eutectic Nb-Si binary alloys, the inter-dendritic eutectic structure consists of niobium rods and plates dispersed in the Nb_3Si intermetallic matrix.[29] This would also confirm the Phase-Field results on the morphology of the eutectics reported by Lewis et al.[27] that higher volume fractions of the second phase would result in the plate-like morphologies. In the present simulation, a periodic boundary condition is maintained and the solid-liquid interface thickness is taken as 0.175 μm which corresponds to 3.5 grid points. The Phase-Field methodology needs the diffuse interface thickness to be at least 3–4 grid points for its numerical stability. The effect of the process parameters and physical quantities on the eutectic solidification is currently being studied and will be reported subsequently.

4. Summary

Multicomponent Nb-Si composites are regarded as potential future candidates for the aero-engine components. In the present study, Phase-Field modeling using MICRESS has been performed on the binary Nb-16 at.% Si alloy to understand the microstructural evolution of Nb(Si) and the eutectic Nb_3Si phase. The effect of the heat extraction that manifests as cooling rates, results in a finer microstructure with increased heat extraction rates. The same is seen with lower solute diffusivity in the solid. Coring is observed for the cases of lower solute diffusivity in the solid. Using MICRESS, it was possible to simulate the dendritic solidification followed by eutectic solidification in one simulation due to its ability to represent multiple phase transformations. The modeling of subsequent eutectoid transformation after solidification resulting in eutectoid Nb_5Si_3 phase will be reported subsequently.

Acknowledgments

The authors acknowledge Christine Furstoss and Craig Young for providing their valuable suggestions on the project, Dr. Bernd Böttger and Philippe Schaffnit for their advise on the technical details associated with implementation of MICRESS software.

References

1. B.P. Bewlay, M.R. Jackson, and M.F.X. Gigliotti, Niobium Silicide High Temperature, *Situ Composites, Intermetallic Compounds—Principles and Practice*, Vol. 3, R.L. Fleischer and J.H. Westbrook, Eds., John Wiley & Sons, 2001, p 541
2. P.R. Subramanian, M.G. Mendiratta, D.M. Dimiduk, and M.A. Stucke, Advanced Intermetallic Alloys—Beyond Gamma Titanium Aluminides, *Mater. Sci. Eng. A*, 1997, **239–240**, p 1-13

3. B.P. Bewlay, M.R. Jackson, and P.R. Subramanian, Processing High-Temperature Refractory-Metal Silicide In-Situ Composites, *J. Miner. Met. Mater. Soc.*, 1999, **51**, p 32-36
4. B.P. Bewlay, J.J. Lewandowski, and M.R. Jackson, Refractory Metal-Intermetallic In-Situ Composites for Aircraft Engines, *J. Miner. Met. Mater. Soc.*, 1997, **49**(8), p 44-45, 67
5. B.P. Bewlay, M.R. Jackson, J.-C. Zhao, and P.R. Subramanian, A Review of Very-High-Temperature Nb-Silicide-Based Composites, *Metall. Mater. Trans. A*, 2003, **34**, p 2043-2052
6. B.P. Bewlay, M.R. Jackson, J.-C. Zhao, P.R. Subramanian, M.G. Mendiratta and J.J. Lewandowski, *MRS Bull*, 2003, p 646
7. B.P. Bewlay, M.R. Jackson, and R.R. Bishop, The Nb-Ti-Si Ternary Phase Diagram: Determination of Solid-State Phase Equilibria in Nb- and Ti-Rich Alloys, *J. Phase Equilibria*, 1998, **19**(6), p 577-586
8. B.P. Bewlay, J.A. Sutliff, and R.R. Bishop, Evidence for the Existence of Hf_5Si_3, *J. Phase Equilibria*, 1999, **20**(2), p 109-112
9. J.-C. Zhao, B.P. Bewlay, M.R. Jackson, and L.A. Peluso, Alloying and Phase Stability in Niobium Silicide In-Situ Composites, *Structural Intermetallics 3rd International Symposium*, K.J. Hemker and D.M. Dimiduk, Eds., 2001, TMS, p 483-491
10. H. Liang and Y.A. Chang, Thermodynamic modeling of the Nb-Si-Ti ternary system, *Intermetallics*, 1999, **7**(5), p 561-570
11. LQ Chen, Phase-Field models for microstructure evolution, *Annu. Rev. Mater. Res.*, 2000, **32**, p 113-140
12. Available at http://www.micress.de
13. H.S. Udaykumar and W. Shyy, Development of a Grid-supported Marked Particle Scheme for Interface Tracking, *11th AIAA Comp. Fluid. Dyn. Conf. (Orlando, FL, 1993)*, AIAA-93-3384
14. D. Juric and G. Tryggvason, A Front-Tracking Method for Dendritic Solidification, *J. Comput. Phys.*, 1996, **123**(1), p 127-148
15. A. Karma and W.-J. Rappel, A Phase-Field Method for Computationally Efficient Modeling of Solidification with Arbitrary Interface Kinetics, *Phys. Rev. E*, 1996, **53**(4), p 3017-3020
16. G. Caginalp, Surface Tension and Supercooling in Solidification Theory, *Applications of Field Theory to Statistical Mechanics*, L. Garrido, Ed. Springer-Verlag, Berlin, 1985, p 216
17. A.A. Wheeler, W.J. Boettinger, and G.B. McFadden, Phase-Field Model for Isothermal Phase Transitions in Binary Alloys, *Phys. Rev. A*, 1992, **45**, p 7424-7439
18. R. Kobayashi, Modeling and Numerical Simulations of Dendritic Crystal Growth, *Physica D*, 1993, **63**, p 410-423
19. J.A. Sethian and J. Strain, Crystal Growth, Dendritic Solidification, *J. Comput. Phys.*, 1992, **98**(2), p 231-253
20. W.W. Mullins and R.F. Sekerka, Stability of a Planar Interface During Solidification of a Dilute Binary Alloy, *J. Appl. Phys.*, 1964, **35**(2), p 444-451
21. S.-L. Wang, R.F. Sekerka, A.A. Wheeler, B.T. Murray, S.R. Coriell, R.J. Braun, and G.B. McFadden, Thermodynamically-Consistent Phase-Field Models for Solidification, *Physica D*, 1993, **69**(1–2), p 189-200
22. A. Karma and W.-J. Rappel, Quantitative Phase-Field Modeling of Dendritic Growth in Two and Three Dimensions, *Phys. Rev. E.*, 1998, **57**(4), p 4323-4349
23. I. Steinbach, F. Pessolla, B. Nestler, M. Seeßelberg, R. Prieler, G.J. Schmitz, and J.L.L. Rezende, A Phase Field Concept for Multiphase Systems, *Physica D*, 1996, **94**(3), p 135-147
24. U. Grafe, B. Böttger, J. Tiaden, and S.G. Fries, Simulations of the Initial Transient During Directional Solidification of Multicomponent Alloys Using the Phase Field Method, *Model. Simul. Mater. Sci. Eng.*, 2000, **8**(6), p 871-880
25. A. Karma and W.J. Rappel, Phase-Field Model of Dendritic Side Branching With Thermal Noise, *Phys. Rev. E.*, 1999, **60**(4), p 3614-3625
26. J.H. Jeong, N. Goldenfield, and J.A. Dantzig, Phase Field Model for Three-dimensional Dendritic Growth With Fluid Flow, *Phys. Rev. E*, 2001, **64**(4), p 041602-041615
27. D. Lewis, T. Pusztai, L. Granasy, J. Warren, and W. Boettinger, Phase-Field Models for Eutectic Solidification, *J. Miner. Met. Mater. Soc.*, April 2004, p 35-39
28. B. Böttger, J. Eiken, and I. Steinbach, Phase Field Simulation of Equiaxed Solidification in Technical Alloys, *Acta Mater*, 2006, **54**(10), p 2697-2704
29. K.-M. Chang, B.P. Bewlay, J.A. Sutliff and M.R. Jackson, Cold-Crucible Directional Solidification of Refractory Metal-Silicide Eutectics, *J. Miner. Met. Mater. Soc.*, June 1992, p 59